

# Spatial Augmented Reality for Environmentally-Lit Real-World Objects

Alvin J. Law<sup>1</sup> and Daniel G. Aliaga<sup>2</sup>

Department of Computer Science at Purdue University

## ABSTRACT

One augmented reality approach is to use digital projectors to alter the appearance of a physical scene, avoiding the need for head-mounted displays or special goggles. Instead, spatial augmented reality (SAR) systems depend on having sufficient light radiance to compensate the surface's colors to those of a target visualization. However, standard SAR systems in dark room settings may suffer from insufficient light radiance causing bright colors to exhibit unexpected color shifts, resulting in a misleading visualization. We introduce a SAR framework which focuses on minimally altering the appearance of arbitrarily shaped and colored objects to exploit the presence of environment/room light as an additional light source to achieve compliancy for bright colors. While previous approaches have compensated for environment light, none have explicitly exploited the environment light to achieve bright, previously non-compliant colors. We implement a full working system and compared our results to solutions achievable with standard SAR systems.

**Keywords:** spatial-augmented reality, projector-based displays, interaction design, mobile and ubiquitous visualization.

**Index Terms:** D.2.6 Graphical environments; H.5.1 Artificial, augmented, and virtual realities.

## 1 INTRODUCTION

Augmented reality systems add computer-controlled content onto real-world scenes to provide an intuitive interface of allowing users to see the physical object or scene augmented with carefully controlled visualizations. Spatial augmented reality (SAR) systems use digital projector light to produce visualizations that alter or augment the appearance of arbitrarily colored and arbitrarily shaped physical objects. These systems enable appearance editing visualizations (AEVs) which allow multiple simultaneous observers to benefit from their natural cues of depth perception and parallax while observing the scene (e.g., [1, 4, 13, 15, 20, 21]).

We focus on enabling a *target* AEV in a diffuse *scene* containing unspecified environment lighting and without the guarantee of having sufficient projector light radiance. Supporting unspecified environment light simplifies deployment of an SAR system and also broadens its range of possible uses. However, supporting unspecified lighting as well as arbitrarily shaped and colored objects only exacerbates the spectrally-dependent problem of ensuring sufficient projector light radiance is present to make the desired appearance changes. How accurately an AEV's colors can be achieved is called the AEV's *compensation compliancy*. Compensation compliancy is critical – inaccurately compensated surfaces may lead to misleading visuals.

Since adding additional projectors is impractical, compensation compliancy for a static scene can be improved with only two strategies. First, the amount of light radiance available can be

maximized by altering the projectors' positions to minimize the distance and angular attenuation of projector light radiance (e.g., [11]). Second, the target's colors can be altered to a similar as possible set of colors that requires less light radiance to be satisfactorily achieved. The former case does not guarantee the target visualization will become compliant. Thus, the latter case is the only way to guarantee a compliant visualization for when there is fundamentally insufficient projector light radiance. The change in colors, however, must be minimal such that the intent of the visualization is conveyed as best as possible. Our approach uses the second methodology for improving SAR systems.

A key observation for our method is that the environment light in a lit room can be exploited as an additional source of light radiance in order to achieve the same bright colors which would otherwise have been non-compliant in a dark room. Most previous SAR systems operate in the ideal condition of dark rooms with no environment light and/or simply assume enough projector light radiance is provided. Further, unlike prior SAR systems which tolerate the presence of environment light, we exploit environment light as a benefit for achieving brighter colors.

Our appearance modification process simultaneously modifies the chrominance and luminance of the target visualization's colors in a spatially varying manner in order to discover an as-similar-as-possible compliant altered appearance (Figure 1). The spatially-varying optimization allows the chrominance and luminance across a target visualization to be locally altered when achieving a compliant visualization. In addition, the optimization attempts to preserve the same color ratios in the altered visualization as in the original target visualization. Thus, despite the initial desire for colors darker than the environment's baseline illumination level, our method is able to obtain a solution with a visual brightness and contrast comparable to that of the original target visualization.

The input to our method is a physical scene of one or more objects, the scene's physical surface albedo image  $A_s(p_i)$ , the scene's environment illumination image  $E(p_i)$ , and a target AEV  $T(p_i) = A_t(p_i)S(p_i)$ .  $A_s$ ,  $E$ , and  $T$  are defined for all surface points  $p_i$  visible from the camera.  $A_s$  contains an estimation of the scene's surface albedo when illuminated by both the maximal amount of projector illumination and the environment light.  $A_t$  contains the target AEV's colors with no shading effects.  $S$  is the target AEV's shading model (e.g., a diffuse or specular material illuminated by a set of virtual lights). We assume the  $A_s$  and  $A_t$  albedo images each consist of constant-colored regions; however, the AEV can have color gradients due to shading and illumination from  $S$ .  $E$  is a photograph of the scene illuminated by any source of environment light. The output of our method is a modified, compliant AEV  $T_c(p_i) = A_c(p_i)S(p_i)$  where  $A_c$  is a modified, compliant albedo image and  $S$  is the same target shading model.

We have implemented a prototype system and compare our results to those achieved using a standard SAR system in both a dark room environment and a lit room environment. In all cases, our AEV demonstrates improved compliancy without sacrificing the intent of the original visualization.

<sup>1</sup>ajlaw@cs.purdue.edu

<sup>2</sup>aliaga@cs.purdue.edu

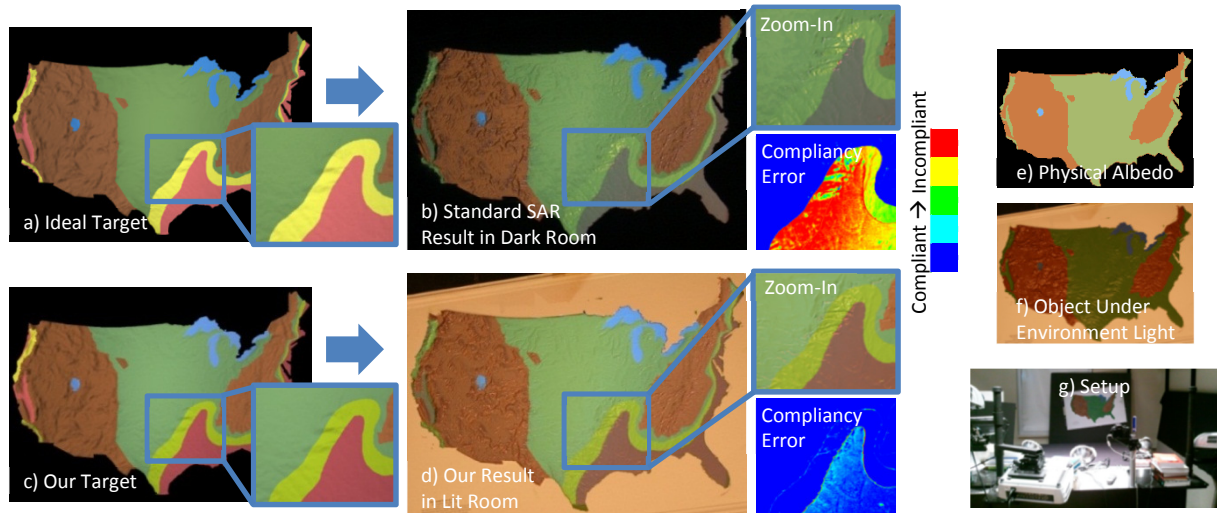


**Figure 1. Spatial Augmented Reality for Environmentally-Lit Real-World Objects.** The compensation compliancy of an appearance editing visualization (AEV) is improved with the presence of environment light and our appearance optimization. This visualization represents US regions in danger of flooding due to increasing sea levels. a) Image of the inconformant ideal target visualization and a zoom-in region. b) Photograph of an inconformant AEV using the ideal target and a standard dark room SAR system. The red and yellow colors are faded, and the yellow color is blending in with the green color. The visualization depicts the compliancy of the zoom-in region (blue to red in increasing inconformity). c) Image of our modified and similar target visualization. d) Photograph of a conformant AEV in a lit room using the modified target. This more conformant AEV contains more accurately reproduced colors. e) Image of the physical albedo of the map. f) Photograph of the map under the environment light used. g) Photograph of the appearance editing setup.

## 2 RELATED WORK

Most prior SAR systems address the computation of compensation images without addressing an appearance’s compliancy – the target visualizations are assumed to be conformant or projected on white/near-white objects (e.g., [4, 15, 21]). Sheng et al. [17] and Bai et al. [3] address the cancellation of inter-reflections and other global illumination effects to improve compensation quality, but they do not guarantee a target appearance to be conformant.

SAR systems which discuss improving the compliancy of target visualizations assume a dark room setup exists (e.g., [1, 11, 12]). Law et al. [12] alter a target visualization’s colors to improve its compliancy. However, they assume a dark room and would not produce conformant results for colors dimmer than the environment’s baseline illumination. Also, their work only considers a single point to represent each arbitrarily large patch. However, in a lit room a patch can be a complex mixture of conformant, inconformant due to too much light radiance, and inconformant due to too little light radiance. Our method uses multiple points per patch in order to accurately represent a patch’s varying compliancy types.

Our appearance optimization is a gamut mapping which alters a set of inconformant visualization colors to a set of conformant colors. Gamut mapping methods analyze either color data (e.g., [5, 9]) and/or the spatial relationship between colors (e.g., [10, 22]). Similarly, our method considers the surface albedo, target colors, and amount of environment light. However, unlike gamut mapping, we also seek to ensure/improve the explicit ability to produce a target AEV. For strong appearance changes, our method takes a significant step further by striving to balance the change of intended colors, maintain color contrast, and achieve compliancy.

SAR systems use radiometric calibration to improve the accuracy of compensated colors (e.g., [7, 8, 14, 16, 19]). However, radiometric calibration alone may be insufficient for achieving compliancy with significant alterations because it typically assumes sufficient light radiance. A few prior radiometric calibration works have partially addressed our targeted problem. Wang et

al. [18] assumed no environment light and performed a global optimization to obtain a single scalar for compressing target contrast, and Ashdown et al. [2] performed a luminance re-mapping. Fujii et al. [6] adapted to both geometric and photometric changes of the scene and environment. However, the focus was the accuracy of the compensated colors – compliancy was not addressed. In contrast, our method considers the shape of the projection surface, the spatial relationship between the target colors, the target colors’ chrominance and luminance, the presence of unspecified environment light, and ensures compensation compliancy.

## 3 COMPENSATION COMPLIANCY WITH ENVIRONMENT LIGHT

Ensuring compensation compliancy in a lit room requires a model of the gamut of conformant colors for any given surface point. We approximate the total amount of light radiance reflected from an object point  $p_i$  on a diffuse surface as:

$$\tilde{L}(p_i) = A_s(p_i) \sum_j^P \frac{L_{max}(n_i \cdot l_j)}{d_{ij}^2} \quad (1)$$

where  $L_{max}$  is the maximum projector luminance,  $(n_i \cdot l_j)$  represents the angular attenuation ( $l_j$  is the directional vector to projector  $j$  in a setup with  $P$  projectors, and  $n_i$  is the surface normal), and  $1/d_{ij}^2$  represents the distance attenuation from projector  $j$  to  $p_i$ . Environment light  $E(p_i)$  is already factored into  $A_s(p_i)$  because, in practice, it is impractical to capture a photograph containing only the physical albedos. Object point  $p_i$  is deemed conformant if  $E(p_i) \leq A_t(p_i)S(p_i) \leq \tilde{L}(p_i)$ . Since our method modifies  $A_t$ , we isolate  $A_t(p_i)$  and obtain:

$$E(p_i)/S(p_i) \leq A_t(p_i) \leq \tilde{L}(p_i)/S(p_i) \quad (2)$$

The compliancy band  $B_i$  of point  $p_i$  is a geometric representation of Equation 2. We use CIELAB space to separately alter chrominance and luminance and to approximately measure perceptual differences. For a color  $(L^*, a^*, b^*)$ , the 2D manifolds  $M_e(a^*, b^*)$  and  $M_p(a^*, b^*)$  represent the minimal and maximal luminance thresholds. Each manifold is constructed by sampling

$a^*$  and  $b^*$  across their ranges and computing the luminance  $L_{uv}^*$  for each sampled ( $a_u^*, b_v^*$ ) chrominance. To compute  $M_e$ , each  $L_{uv}^*$  is initialized to 0 and iteratively increased until its RGB equivalent is compliant.  $M_p$  samples are similarly computed starting at  $L_{uv}^* = 100$  and decreased until compliance. Now,  $E(p_i) \leq M_e$  and  $M_p \leq A_s(p_i)$ . Lastly, each  $L_{uv}^*$  sample value in  $M_e$  is divided by  $S(p_i)$ .  $M_p$  is modified with a per-sample multiplication by the summation in Equation 1 and a per-sample division by  $S(p_i)$ .

Two functions are used to measure the compliancy of target albedo color  $t_i$  at  $p_i$ :  $C_i(t_i)$  and  $D_i(t_i)$ .  $C_i$  yields a scalar by comparing  $t_i[L^*]$  ( $t_i$ 's luminance) to those of  $M_{ei}$  and  $M_{pi}$  at the same ( $t_i[a^*], t_i[b^*]$ ) chrominance.  $C_i(t_i) \geq 0$  indicates compliancy,  $C_i(t_i) < 0$  implies incompliance, and  $C_i(t_i)$ 's magnitude is the degree of compliancy/incompliance.  $D_i$  is the weighted Euclidean distance between  $t_i$  and the closer of  $B_i$ 's compliancy thresholds, with weights ( $w_{L^*}, w_{a^*}, w_{b^*}$ ) allowing a different importance per color space axis.

#### 4 APPEARANCE EDITING PATCHES

Given compliancy bands, the scene's surfaces are partitioned into appearance editing patches with up to  $N$  points representing the varying compliancy across each patch. Patches are regions on the scene's surfaces which have the same color both in  $A_s$  and in  $A_t$ . While  $A_t$  is user defined and thus easily has flat-shaded colors,  $A_s$  is computed by taking a picture of the object under maximal projector illumination from the same viewpoint as  $A_t$  and performing color segmentation (e.g., mean shift segmentation). The multiple points per patch are selected by dividing the patch into bins, computing the compliancy function  $C$  for a random point per bin, and extracting a regular sampling of  $N$  points on  $C$ .

#### 5 APPEARANCE OPTIMIZATION

The appearance optimization uses gradient descent to iteratively alter each patch's color in  $A_t$  so as to produce a set of compliant colors in  $A_c$  (and thus  $T_c$ ). The solution balances the desire for incompliant colors to converge to their nearest compliant colors with the desire to maintain the contrast between the target colors.

##### 5.1 Gradient Descent Methodology

For iteration  $m$ , patch  $k$ 's color  $c_{km}$  is moved in a direction which improves compliancy. This move is done by adding to patch color  $c_{km}$  a CIELAB space color specific to patch  $k$ 's color. Thus,

$$c_{k(m+1)} = c_{km} + s_{km} \quad (3)$$

and the desired color shift  $s_{km} = \{s_{kml^*}, s_{kma^*}, s_{kmb^*}\}$  is:

$$s_{km} = t_{km} - c_{km} \quad (4)$$

where  $t_{km}$  is a computed closer-to-compliant target color for patch  $k$  during iteration  $m$ . In practice, there exist multiple  $t_{km}$ 's per patch (i.e., one target color during iteration  $m$  of a representative point in bin  $f$  of patch  $k$ , or  $t_{fkm}$ ) but still a single  $s_{km}$  must be mutually agreed upon by all representative points per patch. Each  $t_{fkm}$  is a small shift along its gradient  $g_{fkm}$  of  $D_{fk}(c_{km})$ :

$$t_{fkm} = \begin{cases} c_{km} - z g_{fkm} & \text{if patch } k \text{ is incompliant,} \\ c_{km} + z g_{fkm} & \text{if patch } k \text{ is barely compliant.} \end{cases} \quad (5)$$

$z$  controls the rate of change of  $c_{km}$  (we typically use  $z = 0.05$ ).

##### 5.2 Linear Optimization

During each iteration  $m$  and for each color  $c_{km}$ , a linear optimization is used to calculate each  $s_{km}$ . The color shift is chosen so as to achieve a balanced combination of bringing  $c_{km}$  closer to compliancy (*patch equations*) and maintaining the original relative

contrast between different patch colors (*pair equations*).

Patch equations seek to find the most perceptually similar compliant color to  $c_{km}$ . Three equations per patch point (i.e., one for each color channel) are used and are defined as:

$$\alpha_k = \left( (R_k Q_k^v)^{-1} \sum_{i=1}^G Q_i^v \right) \quad (6)$$

$$\alpha_k s_{km} = \alpha_k (t_{fkm} - c_{km}) \quad (7)$$

where  $G$  is the total number of patches,  $R_k$  is the number of selected points from patch  $k$ ,  $Q_k/Q_i$  are the total number of points in patch  $k$ /patch  $i$ , and  $\alpha_k$  is a weight for patch importance with  $v$  being an exponent for indicating patch importance by size.

Pair equations aim to preserve the relative contrast between any two patch's colors  $c_{k_1m}$  and  $c_{k_2m}$ . We define the initial color ratio between two patches and for all color channels to be  $R_{k_1k_2} = c_{k_10}/c_{k_20}$  and a multiplicative weight  $\Omega_{k_1k_2} = d_{k_1k_2}/d_{max}$  where  $d_{k_1k_2}$  is the distance between patches  $k_1$  and  $k_2$  and  $d_{max}$  is the maximum distance between any two patches. Altogether, the per patch pair equation can be written as:

$$\Omega_{k_1k_2} (c_{k_1m} + s_{k_1m}) = \Omega_{k_1k_2} R_{k_1k_2} (c_{k_2m} - s_{k_2m}). \quad (8)$$

#### 6 RESULTS AND DISCUSSION

We have applied our method to create several AEVs. Our camera-projector system extends the radiometric calibration approach in Aliaga et al. [1] and Nayar et al. [14] to use photographs taken with environmental lighting. The environment illumination photograph  $E$  is captured with the same camera parameters used during radiometric calibration. The environment light was supplied by overhead room fluorescent lights plus 2-3 spotlights. Our shown AEVs take approximately 30-60 minutes of compute time. The chosen weights for  $D$ ,  $w_{L^*} = 5$ ,  $w_{a^*} = 2$ , and  $w_{b^*} = 1$ , discourage reduction in luminance, exploit color constancy and produce perceptually more similar appearances.

Figure 1 presents an AEV using a map of the United States. The visualization represents the regions at risk of flooding due to rising sea levels. Without improving its compliancy, the colors of the naive, incompliant AEV are misleading. Figure 1a shows an image of the incompliant ideal target visualization and a zoom-in region on the map. Figure 1b contains a photograph of the AEV of the ideal target using a standard SAR system in a dark room. The zoom-in region is shown on the right along with a visualization of the AEV's compliancy (incompliance increases from blue to red). The red and yellow colors of the AEV are clearly faded, and the yellow color in particular is blending in with the adjacent green color. Figure 1c shows an image of our similar, compliant target visualization to be applied in our environmentally-lit room. A photograph of our more compliant AEV is shown in Figure 1d – the separation of the yellow and green colors is clearly more evident. Figure 1e shows an image of the map's surface albedo. Figure 1f shows a photograph of the map under the environment light used. Figure 1g shows the hardware setup.

Figure 2 uses a car object to demonstrate another improved AEV. The ideal target visualization (Figure 2a) includes yellow lines representing the car aerodynamics. In a dark room, applying the ideal target yields an AEV where some yellow lines fade into the green color of the car (Figure 2b, a zoom-in region and an associated visualization similar to those of Figure 1 are also shown). Our modified target visualization is shown in Figure 2c, and our AEV in a lit room is in Figure 2d. The compliancy of the visualization is improved while the contrast between the green and yellow colors is maintained.

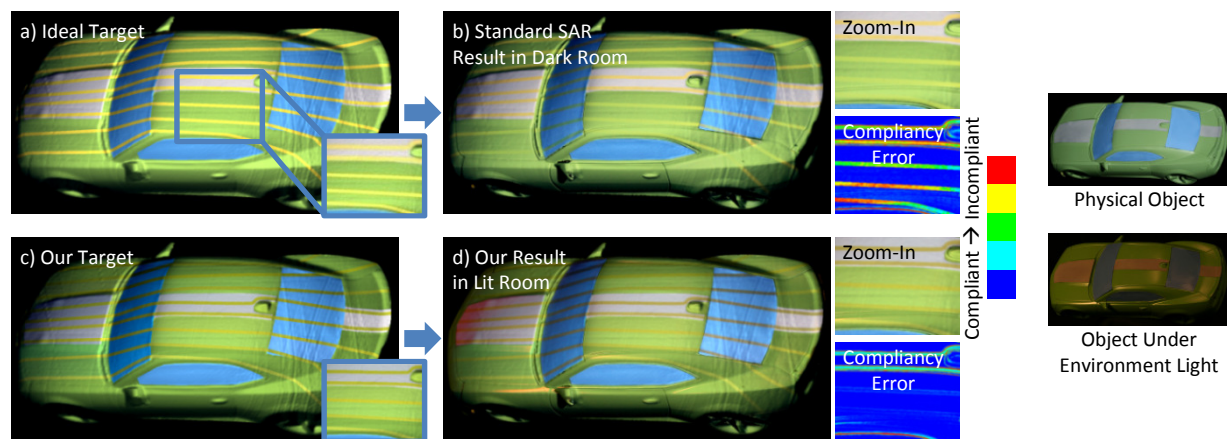


**Figure 2. Car Aerodynamics AEV.** Visualization of a car's aerodynamic behavior. a) Image of the ideal target visualization. b) Photograph of the ideal target AEV in a dark room. The incompliant yellow lines blend into the car's colors. c) Image of our modified target visualization. d) Photograph of our modified target AEV in a lit room. The right is a close-up visualization of the AEV's compliancy (same color scheme as in Figure 1). The aerodynamic lines are most compliant in our solution while maintaining the original relative contrast.

## 7 CONCLUSIONS AND FUTURE WORK

We have presented an extended SAR system which enables achieving compliant AEVs of physical objects with the addition of environment light as a source of light radiance. Our appearance optimization modifies the colors of the target visualization to a best set of similar compliant colors. We consider the introduction of environment light as a way to enable compelling AEVs typically containing more bright colors than dark colors.

The main limitations of our work include the assumptions that the scene's surfaces are diffuse and the scene's surfaces and the target albedo can be divided into regions of nearly constant color. Also, our method does not work well for visualizations where exact colors bear meaning (e.g., a jet-colored mapping).

## ACKNOWLEDGMENTS

We are grateful to our reviewers and to funding provided by NSF CNS 0913875.

## REFERENCES

- [1] D. Aliaga, A. Law, and Y. Yeung, "A Virtual Restoration Stage for Real-World Objects", *ACM Trans. on Graphics*, 27:5, 2008.
- [2] M. Ashdown, T. Okabe, I. Sato, and Y. Sato, "Robust Content-Dependent Photometric Projector Compensation", *Proc. of IEEE International Workshop on Projector Camera Systems*, 2006.
- [3] J. Bai, M. Chandraker, T. Ng, and R. Ramamoorthi, "A Dual Theory of Inverse and Forward Light Transport", *Proc. of IEEE Int'l Conference on Computer Vision*, 2010.
- [4] O. Bimber, D. Iwai, G. Wetzstein, A. Grundhöfer, "The Visual Computing of Projector-Camera Systems", *Computer Graphics Forum*, 27(8), 2219-2245, 2008.
- [5] G. Braun and M.D. Fairchild, "General-Purpose Gamut Mapping Algorithms: Evaluation of contrast-Preserving Rescaling Functions for Color Gamut Mapping", *Proc. of IS&T/SID's 7th Color Imaging Conf.*, 167-172, 1999.
- [6] K. Fujii, M.D. Grossberg, and S.K. Nayar, "A Projector-Camera System with Real-Time Photometric Adaptation for Dynamic Environments", *Proc. IEEE Conf. on Computer Vision and Pattern Recognition*, 1, 814-821, 2005.
- [7] M.D. Grossberg, H. Peri, S.K. Nayar, and P.N. Belhumeur, "Making One Object Look Like Another: Controlling Appearance using a Projector-Camera System", *Proc. of IEEE Conf. on Computer Vision and Pattern Recognition*, 1:452-459, 2004.
- [8] A. Grundhöfer and O. Bimber, "Real-time Adaptive Radiometric Compensation", *IEEE Trans. on Visualization and Computer Graphics*, 14:1, 97-108, 2008.
- [9] C. Hung-Shing, M. Omamiyuda, and H. Kotera, "Adaptive Gamut Mapping Method Based on Image-to-Device", *Proc. of IS&Ts INP 15, Intl. Conf. on Digital Printing Technologies*, 346-349, 1999.
- [10] R. Kimmel, D. Shaked, M. Elad, and I. Sobel, "Space-Dependent Color Gamut Mapping: A Variational Approach", *IEEE Trans. on Image Processing*, 14:5, 796-803, 2005.
- [11] A. Law, D. Aliaga, and A. Majumder, "Projector Placement Planning for High Quality Visualizations on Real-World Objects", *IEEE Trans. on Visualization and Computer Graphics*, 16:6, 1633-1641, 2010.
- [12] A. Law, D. Aliaga, B.Sajadi, A. Majumder, Z. Pizlo, "Perceptually-Based Appearance Modification for Compliant Appearance Editing", *Computer Graphics Forum*, 30:8, 2288-2300, 2011.
- [13] P. Lincoln, G. Welch, and H. Fuchs, "Continual Surface-Based Multi-Projector Blending for Moving Objects", *Proc. of IEEE Virtual Reality*, 115-118, 2011.
- [14] S.K. Nayar, H. Peri, M.D. Grossberg, and P.N. Belhumeur, "A Projection System with Radiometric Compensation for Screen Imperfections", *Proc. of ICCV Workshop on Projector-Camera Systems*, 2003.
- [15] R. Raskar, G. Welch, K.L. Low, D. Bandyopadhyay, "Shader Lamps: Animating Real Objects With Image-Based Illumination", *Proc. of Eurographics Workshop on Rendering Techniques*, 89-102, 2001.
- [16] B. Sajadi, M. Lazarov, and A. Majumder, "ADICT: Accurate Direct and Inverse Color Transformation", *Proc. of European Conference on Computer Vision*, 6314, 72-86, 2010.
- [17] Y. Sheng, T.C. Yao, and B. Cutler, "Global Illumination Compensation for Spatially Augmented Reality", *Computer Graphics Forum*, 29:2, 387-296, 2010.
- [18] D. Wang, I. Sato, T. Okabe, and Y. Sato, "Radiometric Compensation in a Projector-Camera System Based on the Properties of Human Vision System" *Proc. of IEEE International Workshop on Projector Camera Systems*, 2005.
- [19] G. Wetzstein and O. Bimber, "Radiometric Compensation Through Inverse Light Transport", *Proc. of Pacific Graphics*, 391-399, 2007.
- [20] T.C. Yapo, Y. Sheng, J. Nasman, A. Dolce, E. Li, and B. Cutler, "Dynamic Projection Environments for Immersive Visualization", *Proc. of IEEE International Workshop on Projector Camera Systems*, 2010.
- [21] T. Yoshida, C. Horii, and K. Sato, "A Virtual Color Reconstruction System for Real Heritag with Light Projection", *Proc. Int'l. Conf. on Virtual Systems and Multimedia*, 825-831, 2003.
- [22] P. Zolliker and K. Simon, "Retaining Local Image Information in Gamut Mapping Algorithms", *IEEE Trans. on Image Processing*, 16:3, 664-672, 2007.